PNAS
www.pnas.org

Supplementary Information for

Low-Temperature Gas-Phase Formation of Cyclopentadiene and Its Role in the Formation of Aromatics in the Interstellar Medium

Zhenghai Yang[a], Iakov A. Medvedkov[a], Shane J. Goettl[a], Anatoliy A. Nikolayev[b], Alexander M. Mebel[c], Xiaohu Li[d,e]*, Ralf I. Kaiser[a]*

[a]Department of Chemistry, University of Hawai'i at Manoa, Honolulu, HI 96822, USA
[b]Samara National Research University, Samara 443086, Russia
[c]Department of Chemistry and Biochemistry, Florida International University, Miami, Florida 33199, USA
[d]Xinjiang Astronomical Observatory, Chinese Academy of Sciences, Urumqi, Xinjiang 830011, P. R. China
[e]Key Laboratory of Radio Astronomy, Chinese Academy of Sciences, Urumqi, Xinjiang 830011, P. R. China

Correspondence to: Prof. Dr. Ralf I. Kaiser: ralfk@hawaii.edu and Prof. Dr. Xiaohu Li: xiaohu.li@xao.ac.cn

This file includes:

Supplementary Note 1: Alternative pathways in the CH + C_4H_6 reaction.

Multiple pathways to **p1** can be accessed from three-membered cyclic complex(es) **i9** or **i10**, namely, 1) isomerization from both **i9** and **i10** to five-membered cyclic intermediate **i16**; 2) formation of four-membered cyclic **i12** from **i9** through ring expansion and a barrier of 232 kJ mol^{-1} above **i12**; 3) ring-opening to **i15** from **i10**. These pathways to **p1** initiated from **i7** are less competitive considering the high barriers. Three pathways are also revealed in Fig. 4 to the higher energy C_5H_6 isomers **p2** and **p3**, i.e., hydrogen elimination from the CH_2 group of the cyclic $CHCHCH_2$ moieties of **i5, i6,** or **i11** proceeding via exit transition states located 5-18 kJ mol^{-1} above the separated products of **p2** + H and **p3** + H (**i5** → **p2** + H, **i6** → **p3** + H, and **i11** → **p3** + H). However, these three pathways involve high barriers of more than 200 kJ mol^{-1} (205-217 kJ mol^{-1}) and thus are less favorable than the formation of **p1**. More energetically less preferred pathways to **p1** − **p3** including additional intermediates (**i17-i30**) and transition states are depicted in Figure S1.

As shown in Figure S1, the initial complex **i1** can undergo isomerization to **i17** via a submerged barrier of 71 kJ mol^{-1} below the separated reactants prior to cyclization (to a five-membered ring **i21**) and hydrogen shift forming **i16**. The initial insertion intermediates **i2** or **i3** can directly isomerize to **i23** or **i26**, two conformers which are connected through rotational transition state lying only 6 kJ mol^{-1} above **i26**. Three-membered ring opening accompanied with hydrogen migration in **i6** lead to **i18** which initiates a multi-step isomerization pathway to **i26** involving series of acyclic intermediates (**i19**, **i20**, **i22**, **i24-i26**) connected by rotational isomerization and hydrogen migrations pathways (**i19-i20**, **i19-i22**, **i20-i22**, **i22-i24**, **i24-i25**, and **i25-i26**). However, the high barriers of more than 300 kJ mol^{-1} (326 kJ mol^{-1} **i25-i26,** 404 kJ mol^{-1} **i2-i23,** 424 kJ mol^{-1} **i3-i26**) hinder these pathways. **i26** can easily isomerize to **i27** followed by a ring closure producing **i30** which can proceed either via a rearrangement involving a barrier of 150 kJ mol^{-1} to **i16** or via a H loss from the CH_2 group to **p1** over a tight exit transition state of 15 kJ mol^{-1}. As for the pathways to **p2**−**p3**, a hydrogen shift-hydrogen elimination pathway (**i7** → **i29** → **p3** + H) as well as a cyclization-hydrogen elimination (**i25** → **i28** → **p2** + H) pathway are also identified, in which **i28** and **i29** can easily interconvert considering that a barrier of only 17 kJ mol^{-1} separates them. Noted that the barriers for the formation of **i28** or **i29** exceed 200 kJ mol^{-1} (**i19** → **i22** 225 kJ mol^{-1}, **i7** → **i29** 206 kJ mol^{-1}), which hinders the formation of **p2**−**p3**.

Supplementary Note 2: Comparison of the contributions of the channels to cyclopentadiene.

Based on the analysis of the full PES of the 1,3-butadiene + methylidyne reaction we can unambiguously distinguish 9 main exit channels starting from intermediates **i3**, **i21**, **i30**, **i6**, **i7**, **i9**, **i10**, and **i14**, which all lead to 1,3-cyclopentadiene. Except for **i16**, there are also two other five-membered cyclic compounds **i21** and **i30** (Figure S1) that have the cyclopentadiene skeleton, but it should be noted that the pathways involving them are not important as shown in Table S3. RRKM calculations predict that the **i3** → **i15** → **i16** → **p1** + H is channel the most favorable for the formation of **p1** regardless of the initial intermediates. Its yield is nearly 100% if the reaction begins from **i1**, **i2**, or **i3**. This is attributed to the facts that **i1** is metastable and spontaneously collapses to **i3** is below than ***i1*** itself indicating that that rotational isomerizations **i2** → **i3** → **i15** (are more than several orders of magnitude faster than their 3-membered cyclic closures to **i4** and **i5** and the four-membered ring closure of **i3** to **i12**. Alternatively, the **i7** → **i15** → **i16** → **p1** channel makes a quarter of the total contribution to the formation of **p1** of **i4**/**i5** serve as the initial adducts. This is because the barriers for **i4** → **i3** and **i5** → **i2** (67 and 65 kJ mol^{-1}) are comparable with that for **i7** → **i15** (57 kJ mol^{-1}), which results in similar rate constants, 3.26E+11 s^{-1} (**i4** → **i3**), 4.11E+11 s^{-1} (**i5** → **i2**), and 4.08E+11 s^{-1} (**i7** → **i15**). Two other exit channels **i14** → **i15** → **i16** → **p1** + H and **i10** → **i15** → **i16** → **p1** + H are insignificant due to very high barriers, as their rate constants are orders of magnitude lower than those for the ring opening in the three-membered cyclic isomers **i4**, **i5**, and **i7**. The last two pathways **i10** → **i16** → **p1** + H and **i9** → **i16** → **p1** + H involving the three-membered ring expansion of **i9** or **i10** into the five-membered ring of **i16** require even higher barriers to be overcome and are therefore negligible.

To summarize, according to the RRKM calculations the most prevailing channels include the following:

1) **(i1/i2 →) i3 → i15 → i16 → p1** + H

2) **i4 → (i5 → i2 →) i3 → i15 → i16 → p1** + H

3) **i5 → i4/i2 → i3 → i15 → i16 → p1** + H

4) **(i4 →) i5 → i6 → i7 → i15 → i16 → p1** + H

Supplementary Note 3: Astrochemical modeling results.

The rate coefficients of the reactions included in the modeling are mainly derived from the published results. For example, under low-temperature conditions, the rate coefficients for the reaction of methylidyne (CH) with 1,3-butadiene (C_4H_6) is predicted to be around 4×10^{-10} cm^3 $molecule^{-1}$ s^{-1} (*1, 2*), the rate coefficients of CH with other C1, C2, C4 hydrocarbons, and benzene are measured to be $(3\text{-}5)\times10^{-10}$ cm^3 $molecule^{-1}$ s^{-1} (*3-6*). As depicted in Fig. 6A, the predictive capabilities of the astrochemical model can be benchmarked for cyclopentadiene (C_5H_6), cyanocyclopentadiene (C_5H_5CN), and ethynylcyclopentadiene (C_5H_5CCH), with predicted peak abundances of $(8.1 \pm 0.4) \times 10^{-10}$ at 8.0×10^4 years, $(10.2 \pm 0.5) \times 10^{-11}$ at 3.2×10^5 years, and $(2.5 \pm 0.2) \times 10^{-10}$ at 3.2×10^5 years, respectively; these predictions agree well with the astronomically detected fractional abundance of $(8 - 16) \times 10^{-10}$ ((*7, 8*)), $(5 - 16) \times 10^{-11}$ ((*8-11*)), and $(2 - 5) \times 10^{-10}$ ((*9*)) relative to molecular hydrogen. This model reveals that the main pathways to cyanocyclopentadiene (C_5H_5CN) include the CH − C_4H_5CN and CN − C_5H_6; fundamental pathways to ethynylcyclopentadiene (C_5H_5CCH) are C_2H − C_5H_6 and CH − C_4H_5CCH. Considering bicyclic aromatics carrying a five-membered ring (Fig. 6B), abundances of indene (C_9H_8) and cyanoindene (C_9H_7CN) are predicted to be $(9.0 \pm 0.4) \times 10^{-10}$ at 2.5×10^5 years and $(1.1 \pm 0.2) \times 10^{-11}$ at 3.2×10^5 years, while astronomical observations suggest fractional abundances of $(8 - 14) \times 10^{-10}$ and $(1 - 3) \times 10^{-11}$ ((*10, 12*)), respectively. As for the cyano (CN) and ethynyl (CCH) substituted benzene and naphthalene molecules (Fig. 6C-D), modeling predictions of peak abundances of cyanobenzene (C_6H_5CN), ethynylbenzene (C_6H_5CCH), and cyanonaphthalene ($C_{10}H_7CN$) are reported to $(4.2 \pm 0.5) \times 10^{-11}$, $(2.2 \pm 0.3) \times 10^{-10}$, and $(6.0 \pm 0.5) \times 10^{-11}$ thus replicating the astronomical observations nicely ($(4 - 20) \times 10^{-11}$ for C_6H_5CN (*9, 13, 14*), $(2 - 3) \times 10^{-10}$ for C_6H_5CCH(*9*), $(5 - 20) \times 10^{-11}$ for $C_{10}H_7CN$ (*10, 15*)). The peak fractional abundances of the molecular building blocks and hence precursors of the cyclic compounds, i.e. propargyl (C_3H_3), vinylacetylene (C_4H_4), cyanoacetylene (HCCCN), vinyl cyanide (C_2H_3CN), and cyano substituted propylene isomers (C_3H_5CN), are also included in the model. These results are close to the observed data of $(8 - 12) \times 10^{-9}$ ((*16, 17*)), $(1 - 2) \times 10^{-9}$ ((*7, 18*)), $(2 - 20) \times 10^{-9}$ ((*19, 20*)), $(5 - 8) \times 10^{-10}$ ((*18, 21*)), and $(3 - 5) \times 10^{-11}$ (Figure S5-6) thus highlighting the predictive nature of our astrochemical model (Table S6) (*22*). Note that benzene (C_6H_6) and naphthalene ($C_{10}H_8$) are nonpolar and hence cannot be detected via radioastronomical techniques. Nevertheless,

the detected rich abundances of PAHs in TMC-1 indicate that benzene and naphthalene represent an 'invisible' reservoir reacting rapidly with cyano (CN) and ethynyl (CCH) radicals to their substituted proxies (*23, 24*). Here, peak fractional abundances of benzene and naphthalene are predicted to be $(7.5 \pm 0.3) \times 10^{-9}$ and $(4.8 \pm 0.5) \times 10^{-8}$, which are about one to three magnitudes higher than their CN/CCH derivatives.

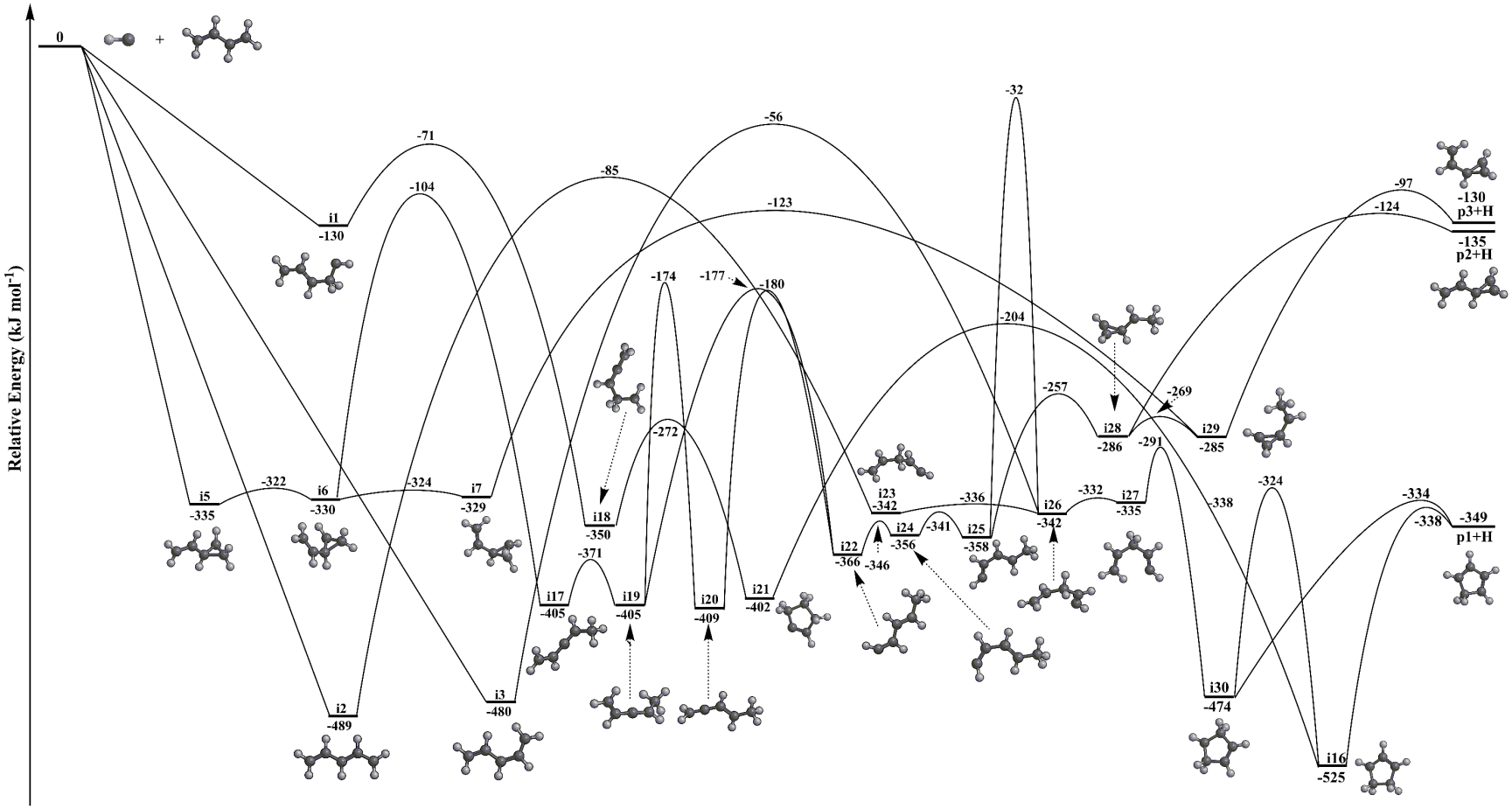

Figure S1. Supplementary PES. Additional pathways to cyclopentadiene (**p1**), trans- (**p2**) and cis-3-vinyl-cyclopropene (**p3**) for the reaction of methylidyne (CH) with 1,3-butadiene (C_4H_6).

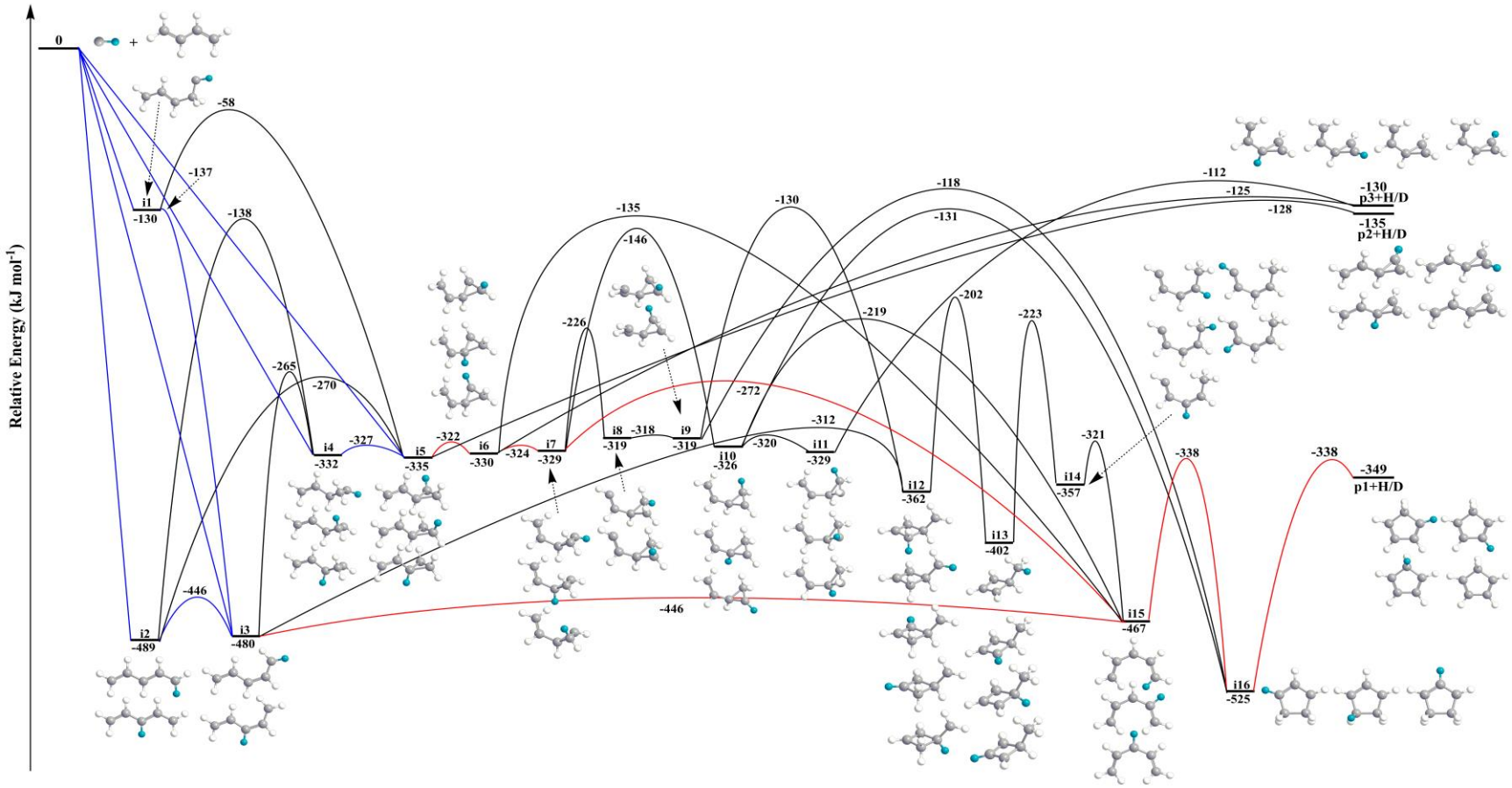

Figure S2. PES of reaction of CD with C_4H_6. Pathways to **p1**, **p2**, and **p3** for the reaction of d1-methylidyne (CD) with 1,3-butadiene (C_4H_6).

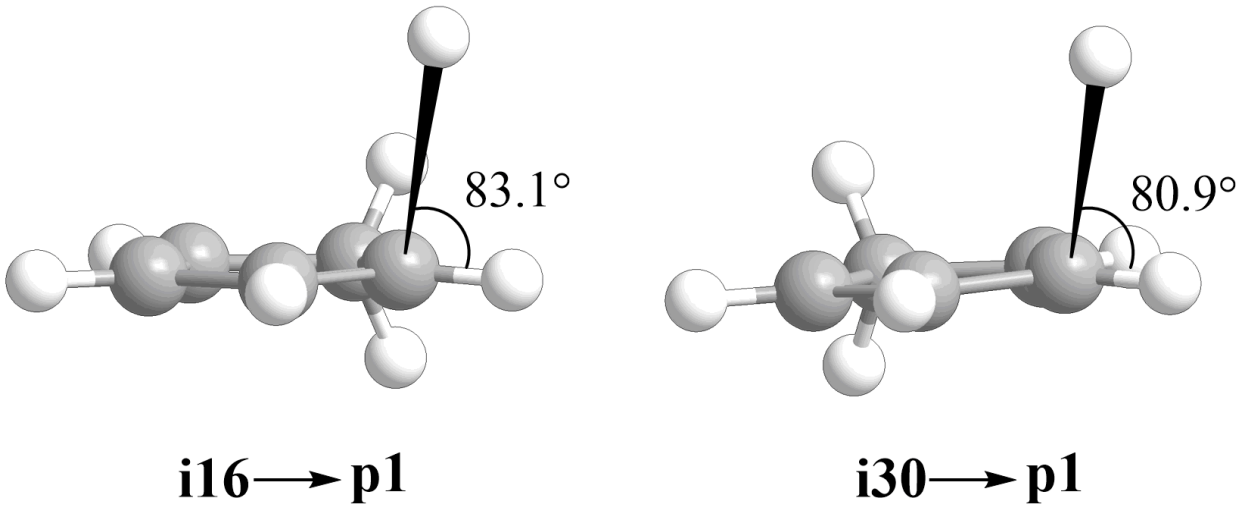

Figure S3. Computed geometries of the exit transition states leading to p1. The computed geometries of exit transtition states of **i16** → **p1** + H and **i30** → **p1** + H.

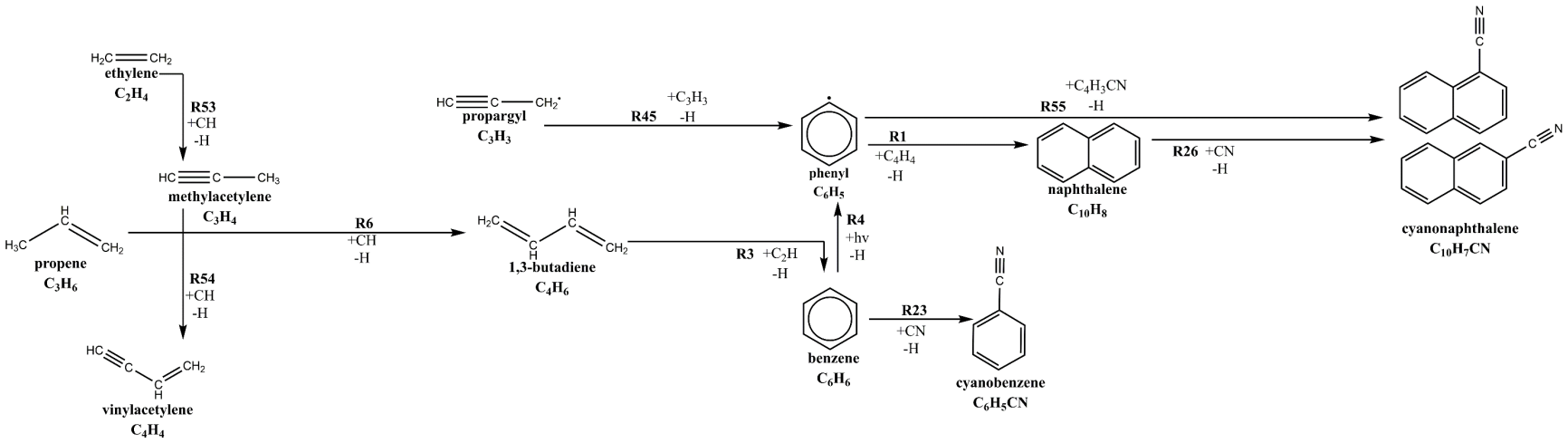

Figure S4. **Previously incomplete reaction network.** The main reactions leading to naphthalene ($C_{10}H_8$) and cyanonaphthalene ($C_{10}H_7CN$) molecules in the previous reaction network. The network derived in the presente work is shown as Figure 5 in the manuscript.

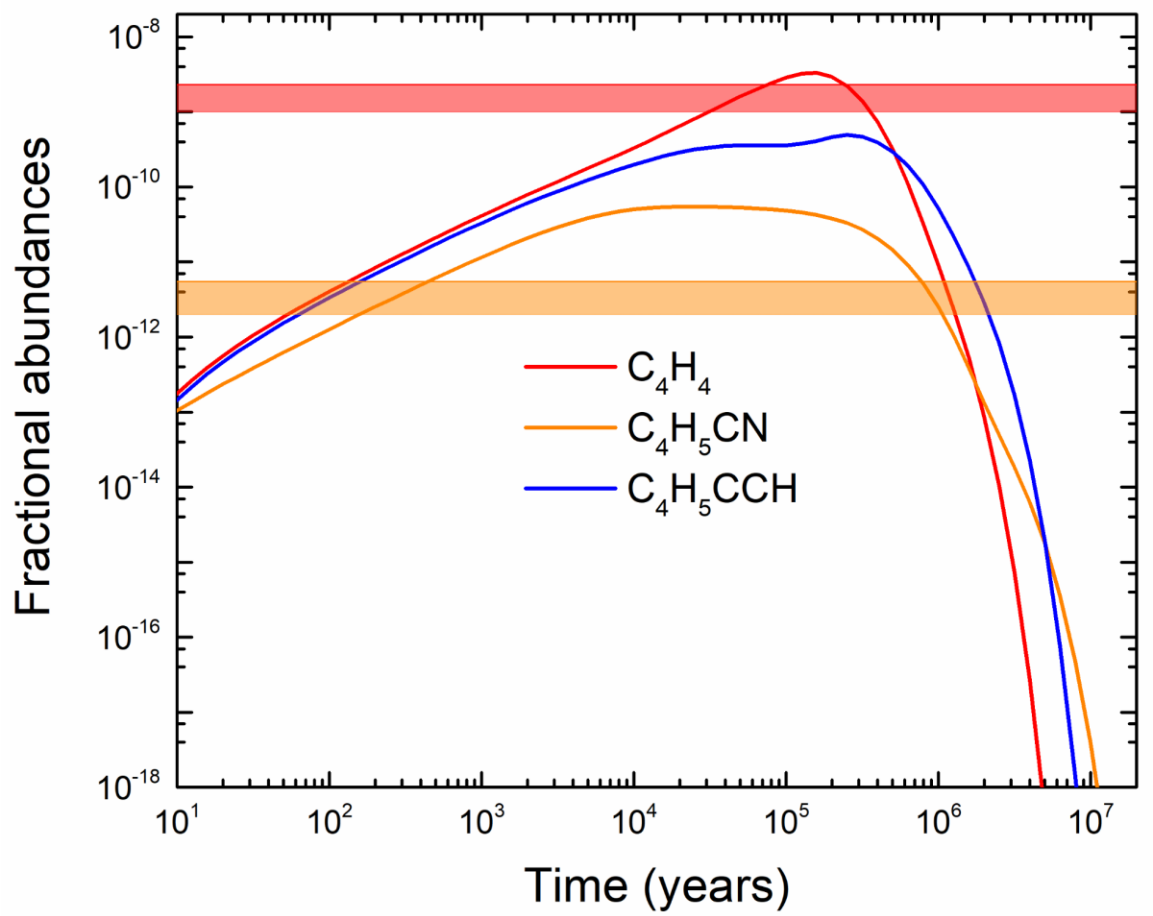

Figure S5. Fractional abundances of small molecules derived from the new astrochemical modeling (II). The fractional abundances of the vinylacetylene (C_4H_4), the cyano and ethynyl substitured 1,3-butadiene namely C_4H_5CN, and C_4H_5CCH are plotted as a function of time. The astronomically observed fractional abundances along with the uncertanities are visualized by the horizontal bars.

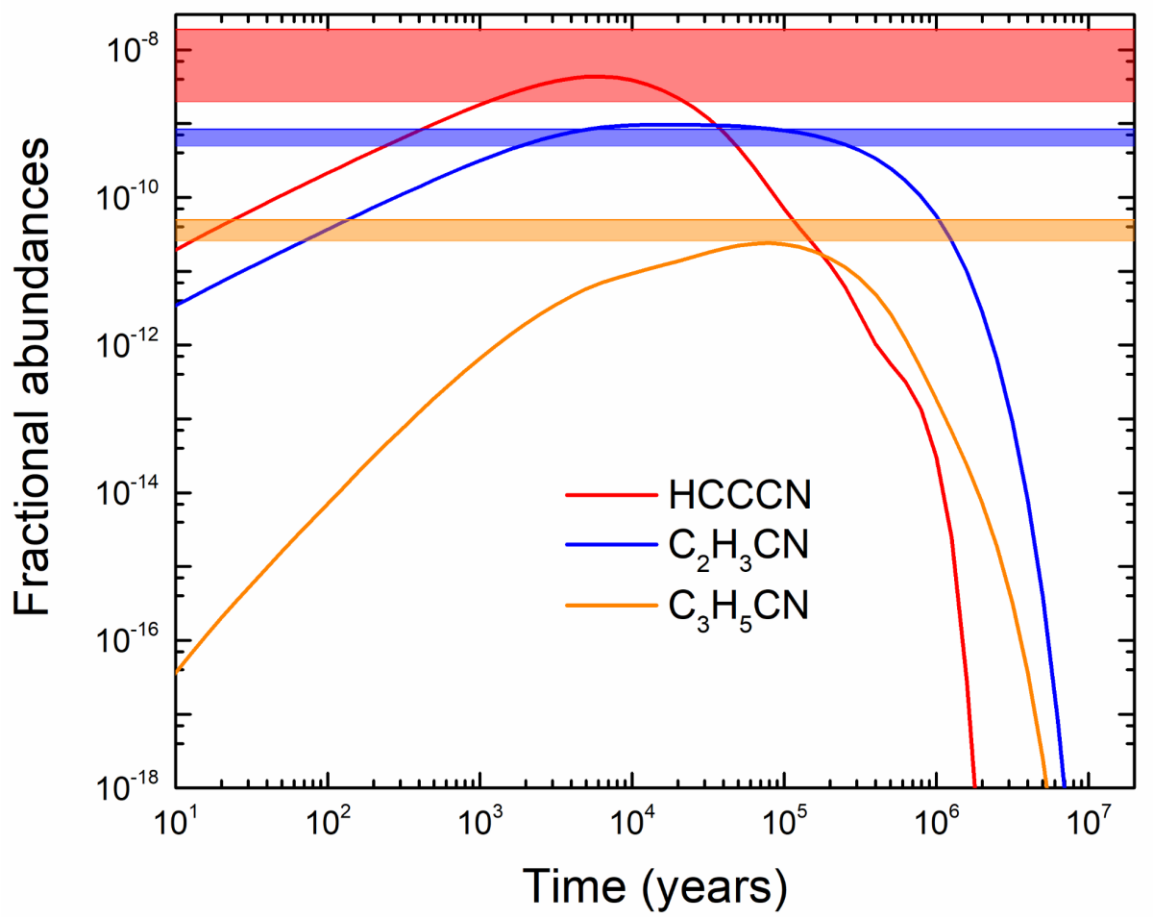

Figure S6. Fractional abundances of small molecules derived from the new astrochemical modeling (III). The fractional abundances of the cyanoacetylene (HCCCN), vinylcyanide (C_2H_3CN), and cyano substituted propylene (C_3H_5CN) are plotted as a function of time. The astronomically observed fractional abundances along with the uncertainties are visualized by the horizontal bars.

Table S1. Peak velocities (v_p) and speed ratios (S) of the methylidyne (CH), d1-methylidyne (CD), and 1,3-butadiene (C_4H_6) reactants along with the corresponding collision energy (E_C) and center-of-mass angle (Θ_{CM}).

Beam	v_p (m s^{-1})	S	E_c (kJ mol^{-1})	Θ_{CM} (deg)
CH	991 ± 22	12.6 ± 0.6		
C_4H_6	445 ± 17	11.1 ± 1.2	6.2 ± 0.3	61.5 ± 0.6
CD	986 ± 19	12.4 ± 0.6		
C_4H_6	445 ± 17	11.1 ± 1.2	6.5 ± 0.3	59.7 ± 0.5

Table S2. Statistical branching ratio (%) to **p1-p3** from initial intermediates of **i1-i5** for the reaction of the methylidyne radical (CH) with 1,3-butadiene ($CH_2CHCHCH_2$) at collision energy (E_c) of 0 and 6.2 kJ mol^{-1}.

E_c		**i1**	**i2**	**i3**	**i4**	**i5**
0	**p1**	76.9	76.9	76.9	76.5	76.5
	p2	0	0	0	0	0
	p3	0	0	0	0	0
6.2	**p1**	75.3	75.3	75.3	74.9	74.9
	p2	0	0	0	0	0
	p3	0	0	0	0.1	0.1

Table S3. Contributions of selected channels for the reaction of 1,3-butadiene+methylidyne with ***i1 – i5*** as initial intermediates at a collision energy E_C of 6.2 kJ mol^{-1}

Main exit channels	***Initial intermediate***				
	i1	***i2***	***i3***	***i4***	***i5***
i3 → i15 → i16 → p1 + H	98.2447%	98.2579%	98.2591%	71.3572%	70.5073%
i7 → i15 → i16 → p1 + H	1.2129%	1.2129%	1.2118%	27.1686%	27.9888%
i14 → i15 → i16 → p1 + H	0.4434%	0.4340%	0.4339%	0.3232%	0.3196%
i10 → i15 → i16 → p1 + H	0.0507%	0.0506%	0.0506%	1.1094%	1.1429%
i30 → (i16) → p1 + H	0.0389%	0.0357%	0.0357%	0.0286%	0.0284%
i21 → i16 → p1 + H	0.0090%	0.0086%	0.0086%	0.0065%	0.0064%
i6 → i15 → i16 → p1 + H	0.0002%	0.0002%	0.0002%	0.0050%	0.0051%
i10 → i16 → p1 + H	0.0000%	0.0000%	0.0000%	0.0003%	0.0003%
i9 → i16 → p1 + H	0.0001%	0.0001%	0.0001%	0.0011%	0.0011%

Table S4. The RRKM rate constants (s^{-1}). The calculated rate constants for H loss channels of CH + C_4H_6 reaction at collision energy of 6.2 kJ mol^{-1}.

	k		*k*		*k*
i2 – i3	5.30E+12	i17 – i21	3.46E+09	i10 – i11	1.13E+13
i3 – i2	3.44E+12	i21 – i17	1.59E+11	i11 – i10	6.64E+12
i3 – i15	2.45E+12	i7 – i10	1.85E+08	i11 – p3	3.53E+07
i15 – i3	5.14E+12	i10 – i7	1.90E+08	i12 – i13	2.71E+08
i15 – i16	2.05E+10	i18 – i6	2.63E+04	i13 – i12	2.65E+08
i16 – i15	2.41E+10	i6 – i18	1.41E+06	i19 – i20	3.60E+07
i16 – p1	8.61E+10	i18 – i19	4.99E+11	i20 – i19	2.07E+07
i1 – i3	1.62E+13	i19 – i18	5.00E+11	i20 – i22	1.81E+08
i3 – i1	1.06E+05	i1 – i5	6.67E+08	i22 – i20	1.94E+09
i16 – i30	7.79E+09	i5 – i1	6.42E+03	i19 – i22	1.48E+07
i30 – i16	4.90E+10	i2 – i18	1.61E+07	i22 – i19	1.83E+08
i2 – i23	3.60E+02	i18 – i2	3.82E+08	i22 – i24	3.88E+12
i23 – i2	8.85E+04	i6 – p3	3.76E+08	i24 – i22	4.81E+12
i23 – i26	2.23E+12	i8 – i9	2.82E+12	i24 – i25	1.71E+14
i26 – i23	2.47E+12	i9 – i8	2.82E+12	i25 – i24	5.96E+13
i26 – i27	1.96E+12	i5 – i6	3.76E+12	i26 – i25	2.91E+01
i27 – i26	2.44E+12	i6 – i5	2.52E+12	i25 – i26	6.79E+00
i27 – i30	7.18E+10	i4 – i3	3.26E+11	i25 – i28	3.69E+10
i30 – i27	4.25E+09	i3 – i4	2.12E+08	i28 – i25	5.47E+11
i30 – p1	4.38E+11	i3 – i26	3.66E+00	i28 – p2	6.90E+07
i7 – i8	7.15E+09	i26 – i3	1.54E+03	i28 – i29	6.66E+11
i8 – i7	1.25E+10	i5 – p2	2.77E+08	i29 – i28	1.03E+12
i1 – i17	3.52E+09	i4 – i5	1.03E+13	i29 – p3	2.19E+08
i17 – i1	7.07E+02	i5 – i4	9.84E+12	i7 – i29	3.93E+06
i16 – i9	2.57E+04	i6 – i7	6.08E+12	i29 – i7	4.69E+06
i9 – i16	3.43E+07	i7 – i6	1.16E+13	i15 – i7	9.11E+08
i16 – i21	3.89E+06	i3 – i18	1.60E+07	i7 – i15	4.08E+11
i21 – i16	1.11E+09	i18 – i3	2.92E+08	i3 – i12	2.12E+09
i9 – i12	1.35E+07	i2 – i5	2.16E+08	i12 – i3	7.65E+11
i12 – i9	1.48E+06	i5 – i2	4.11E+11	i15 – i10	5.82E+07
i16 – i10	1.01E+04	i15 – i6	7.62E+04	i10 – i15	2.68E+10
i10 – i16	7.94E+06	i6 – i15	3.57E+07		
i13 – i14	1.28E+09	i15 – i14	9.31E+09		
i14 – i13	8.28E+08	i14 – i15	1.01E+12		

Table S5. Important bimolecular reactions and photodissociation processes incorporated into the astrochemical model.

Reactant 1	Reactant 2	Products	α	β	γ	No.
C_6H_5	C_4H_4	$C_{10}H_8$+H	4.00E-10	0	0	R1
C_4H_6	C_2	C_6H_5+H	4.00E-10	0	0	R2
C_4H_6	C_2H	C_6H_6+H	4.00E-10	0	0	R3
C_6H_6	hν	C_6H_5+H	3.00E-09	0	3.1	R4
C_2H_2	CN	HCCCN+H	4.00E-10	0	0	R5
C_3H_6	CH	C_4H_6+H	4.00E-10	0	0	R6
C_2H_4	C	C_3H_3+H	4.00E-10	0	0	R7
C_2H_4	hν	C_2H_2+H_2	3.00E-09	0	3.1	R8
C_4H_6	CH	C_5H_6+H	4.00E-10	0	0	R9
C_4H_6	C_3H	C_5H_5CCH+H	4.00E-10	0	0	R10
C_4H_6	C_2N	C_5H_5CN+H	4.00E-10	0	0	R11
C_4H_6	CN	C_4H_5CN+H	4.00E-10	0	0	R12
C_4H_5CN	C_2H	C_6H_5CN+H	4.00E-10	0	0	R13
C_5H_6	CH	C_6H_6+H	4.00E-10	0	0	R14
C_2H_4	CN	C_2H_3CN+H	4.00E-10	0	0	R15
C_5H_6	CH_2CHCC	C_9H_8+H	4.00E-10	0	0	R16
C_5H_6	CN	C_5H_5CN+H	4.00E-10	0	0	R17
C_6H_6	CH	C_5H_5CCH+H	4.00E-11	0	0	R18
C_5H_6	C_2H	C_5H_5CCH+H	4.00E-10	0	0	R19
C_5H_5CN	CH_2CHCC	C_9H_7CN+H	4.00E-10	0	0	R20
C_9H_8	CN	C_9H_7CN+H	4.00E-10	0	0	R21
C_9H_8	CH	$C_{10}H_8$+H	4.00E-10	0	0	R22
C_6H_6	CN	C_6H_5CN+H	4.00E-10	0	0	R23
C_6H_5CN	hν	C_6H_4CN+H	3.00E-09	0	3.1	R24
C_6H_4CN	C_4H_4	$C_{10}H_7CN$+H	4.00E-10	0	0	R25
$C_{10}H_8$	CN	$C_{10}H_7CN$+H	4.00E-10	0	0	R26
C_9H_7CN	CH	$C_{10}H_7CN$+H	4.00E-10	0	0	R27
C_5H_6	C	C_6H_5+H	4.00E-10	0	0	R28
C_5H_5CN	CH	C_6H_5CN+H	4.00E-10	0	0	R29
C_5H_5CN	C	C_6H_4CN+H	4.00E-10	0	0	R30
C_6H_5CCH	hν	C_6H_4CCH+H	3.00E-09	0	3.1	R31
C_5H_5CCH	CH	C_6H_5CCH+H	4.00E-10	0	0	R32
C_5H_5CCH	C	C_6H_4CCH+H	4.00E-10	0	0	R33
C_6H_6	C_2H	C_6H_5CCH+H	4.00E-10	0	0	R34
C_4H_5CN	CH	C_5H_5CN+H	4.00E-10	0	0	R35
C_3H_6	CN	C_3H_5CN+H	4.00E-10	0	0	R36
C_3H_5CN	CH	C_4H_5CN+H	4.00E-10	0	0	R37
C_2H_6	C_2N	C_3H_5CN+H	4.00E-10	0	0	R38
C_3H_6	C_2N	C_4H_5CN+H	4.00E-10	0	0	R39
C_6H_4CCH	C_4H_4	$C_{10}H_7CCH$+H	4.00E-10	0	0	R40
$C_{10}H_8$	C_2H	$C_{10}H_7CCH$+H	4.00E-10	0	0	R41
C_9H_8	C_2H	C_9H_7CCH+H	4.00E-10	0	0	R42
C_9H_7CCH	CH	$C_{10}H_7CCH$+H	4.00E-10	0	0	R43
C_3H_3	C	C_4H_2+H	4.00E-10	0	0	R44
C_3H_3	C_3H_3	C_6H_5+H	4.00E-10	0	0	R45
C_2H_4	C_2H	C_4H_4+H	4.00E-10	0	0	R46
C_2H_6	hν	C_2H_4+H_2	3.00E-09	0	3.1	R47
C_3H_6	C_2H	C_3H_5CCH+H	4.00E-10	0	0	R48
C_3H_5CCH	CH	C_4H_5CCH+H	4.00E-10	0	0	R49
C_4H_5CCH	C_2H	C_6H_5CCH+H	4.00E-10	0	0	R50
C_4H_5CCH	CH	C_5H_5CCH+H	4.00E-10	0	0	R51

C_3H_6	C_3H	C_4H_5CCH+H	4.00E-10	0	0	R52
C_2H_4	CH	C_3H_4+H	4.00E-10	0	0	R53
C_3H_4	CH	C_4H_4+H	4.00E-10	0	0	R54
C_6H_5	C_4H_3CN	$C_{10}H_7CN$	4.00E-10	0	0	R55
C_3H_7	C	C_4H_6+H	4.00E-10	0	0	R56
C_4H_4	CN	C_4H_3CN+H	4.00E-10	0	0	R57
C_3H_5CN	hν	C_3H_4CN+H	3.00E-09	0	3.1	R58
C_3H_7	CN	C_3H_6CN+H	4.00E-10	0	0	R59
C_3H_6CN	C	C_4H_5CN+H	4.00E-10	0	0	R60
C_6H_4	CN	C_6H_3CN+H	4.00E-10	0	0	R61
C_4H_3	CN	C_4H_2CN+H	4.00E-10	0	0	R62
C_4H_4	CN	C_4H_3CN+H	4.00E-10	0	0	R63
C_4H_3CN	hν	C_4H_2CN+H	3.00E-09	0	3.1	R64
C_7H_8	C_2N	C_8H_7CN+H	4.00E-10	0	0	R65
C_8H_8	C_2N	C_9H_7CN+H	4.00E-10	0	0	R66
C_5H_6	C_4H_2CN	C_9H_7CN+H	4.00E-10	0	0	R67
C_6H_3CN	C_3H_5	C_9H_7CN+H	4.00E-10	0	0	R68
C_2H_6	C_3H	C_3H_5CCH+H	4.00E-10	0	0	R69
C_8H_7CN	CH	C_9H_7CN+H	4.00E-10	0	0	R70
C_8H_8	CN	C_8H_7CN+H	4.00E-10	0	0	R71
C_6H_4	C_3H_4CN	C_9H_7CN+H	4.00E-10	0	0	R72

Note: For the neutral-neutral bimolecular reactions, α is the pre-exponential factor with units of s^{-1}. β is dimensionless, representing an empirical parameter which reflects the temperature dependence of α. γ is the factor related to the activation energy with units of K (Kelvin). For cosmic-ray-induced photoreaction, α is the cosmic-ray ionization rate (s^{-1}) normalized to a total rate for electron production from cosmic ray ionization of 1.3×10^{-17} s^{-1} (*25*), ω is the dust-grain albedo in the far ultraviolet. And γ is dimensionless representing the efficiency of cosmic-ray ionization event (*26*).

Table S6. Column density of important C_nH_m, C_nH_mCN, and C_nH_mCCH species in TMC-1. The observed abundances are reported in cited references.

Molecules	N (cm^{-2})	Abundances	References
C_3H_3	8.7×10^{13}	8.7×10^{-9}	a
	$(8\text{-}12)\times10^{13}$	$(8\text{-}12)\times10^{-9}$	b
C_2H_3CN	$(5\text{-}8)\times10^{12}$	$(5\text{-}8)\times10^{-10}$	c
	6.8×10^{12}	6.8×10^{-10}	d
C_4H_4	$(1\text{-}2)\times10^{13}$	$(1\text{-}2)\times10^{-9}$	c, e
HC_3N	$(2.0\text{-}2.5)\times10^{14}$	$(2.0\text{-}2.5)\times10^{-8}$	f
	2.2×10^{13}	2.2×10^{-9}	g
C_3H_5CN	$(3\text{-}5)\times10^{11}$	$(3\text{-}5)\times10^{-11}$	h
C_4H_5CN*[1]	$(2\text{-}5)\times10^{10}$	$(2\text{-}5)\times10^{-12}$	i
C_5H_6	1.3×10^{13}	1.3×10^{-9}	j
	$(8\text{-}16)\times10^{12}$	$(8\text{-}16)\times10^{-10}$	e, k
1-C_5H_5CN	3.1×10^{11}	3.1×10^{-11}	j
	$(12\text{-}16)\times10^{11}$	$(12\text{-}16)\times10^{-11}$	k
	$(7\text{-}10)\times10^{11}$	$(7\text{-}10)\times10^{-11}$	l, m
2-C_5H_5CN	1.3×10^{11}	1.3×10^{-11}	j
	$(1\text{-}2)\times10^{11}$	$(1\text{-}2)\times10^{-11}$	l, m
C_5H_5CCH	$(2\text{-}5)\times10^{12}$	$(2\text{-}5)\times10^{-10}$	j
C_6H_5CN	1.2×10^{12}	1.2×10^{-10}	j
	$(1\text{-}2)\times10^{12}$	$(1\text{-}2)\times10^{-10}$	n
	4×10^{11}	4×10^{-11}	o
	$(7\text{-}26)\times10^{11}$	$(7\text{-}26)\times10^{-11}$	l
C_6H_5CCH	$(2\text{-}3)\times10^{12}$	$(2\text{-}3)\times10^{-10}$	j
C_9H_8	1.6×10^{13}	1.6×10^{-9}	j
	$(8\text{-}14)\times10^{12}$	$(8\text{-}14)\times10^{-10}$	l
	$(8\text{-}10)\times10^{12}$	$(8\text{-}10)\times10^{-10}$	p
2-C_9H_7CN	$(1\text{-}3)\times10^{11}$	$(1\text{-}3)\times10^{-11}$	p
1-$C_{10}H_7CN$	$(2\text{-}11)\times10^{11}$	$(2\text{-}11)\times10^{-11}$	l, q
2-$C_{10}H_7CN$	$(3\text{-}12)\times10^{11}$	$(3\text{-}11)\times10^{-11}$	l, q

*[1] The observed abundance is only for s-*trans*-*E*-1-cyano-1,3-butadiene ($CH_2CHCHCHCN$) isomer, the total abundances are expected to increase sharply with more C_4H_5CN isomers identified in the future.

a) Agúndez, M. et al. Astron. Astrophys. 647, L10 (2021). b) Agúndez, M. et al. Astron. Astrophys. 657, A96 (2022). c) Cernicharo, J. et al. Astron. Astrophys. 647, L2 (2021). d) Minh, Y. C. et al. Astrophys. Space Sci. 175, 165-169 (1991). e) Cernicharo, J. et al. Astron. Astrophys. 663, L9 (2022). f). Cernicharo, J. et al. Astron. Astrophys. 642, L8 (2020). g) Langer, W. D. et al. Astrophys. J. 239, L125 (1980). h) Cernicharo, J. et al. Astron. Astrophys. 663, L5 (2022). i) Cooke, I. R. et al. Astrophys. J. 948, 133 (2023). j) Cernicharo, J. et al. Astron. Astrophys. 655, L1 (2021). k) McCarthy, M. C. et al. Nat. Astron. 5, 176-180 (2021). l) Burkhardt, A. M. et al. Astrophys. J. Lett. 913, L18 (2021). m) Lee, K. L. K. et al. Astrophys. J. Lett. 910, L2 (2021). n) Burkhardt, A. M. et al. Nat. Astron. 5, 181-187 (2021). o) McGuire, B. A. et al. Science 359, 202-205 (2018). p) Sita, M. L. et al. Astrophys. J. Lett. 938, L12 (2022). q) McGuire, B. A. et al. Science 371, 1265-1269 (2021).

References

1. J. Cernicharo *et al.*, TMC-1, the starless core sulfur factory: Discovery of NCS, HCCS, H_2CCS, H_2CCCS, and C_4S and detection of C_5S. *Astron. Astrophys.* **648**, L3 (2021).
2. J.-C. Loison, M. Agúndez, V. Wakelam, E. Roueff, P. Gratier, N. Marcelino, D. N. Reyes, J. Cernicharo, M. Gerin, The interstellar chemistry of C_3H and C_3H_2 isomers. *Mon. Not. R. Astron. Soc.* **470**, 4075-4088 (2017).
3. A. Canosa, I. R. Sims, D. Travers, I. W. M. Smith, B. R. Rowe, Reactions of the methylidine radical with CH_4, C_2H_2, C_2H_4, C_2H_6, and but-1-ene studied between 23 and 295 K with a CRESU apparatus. *Astron. Astrophys.* **323**, 644-651 (1997).
4. J.-C. Loison, A. Bergeat, Rate constants and the H atom branching ratio of the reactions of the methylidyne CH ($X^2\Pi$) radical with C_2H_2, C_2H_4, C_3H_4 (methylacetylene and allene), C_3H_6 (propene) and C_4H_8 (trans-butene). *Phys. Chem. Chem. Phys.* **11**, 655-664 (2009).
5. S. Hamon, S. D. Le Picard, A. Canosa, B. R. Rowe, I. W. M. Smith, Low temperature measurements of the rate of association to benzene dimers in helium. *J. Chem. Phys.* **112**, 4506-4516 (2000).
6. S. Doddipatla *et al.*, Low-temperature gas-phase formation of indene in the interstellar medium. *Sci. Adv.* **7**, eabd4044 (2021).
7. J. Cernicharo, R. Fuentetaja, M. Agúndez, R. I. Kaiser, C. Cabezas, N. Marcelino, B. Tercero, J. R. Pardo, P. de Vicente, Discovery of fulvenallene in TMC-1 with the QUIJOTE line survey. *Astron. Astrophys.* **663**, L9 (2022).
8. M. C. McCarthy *et al.*, Interstellar detection of the highly polar five-membered ring cyanocyclopentadiene. *Nat. Astron.* **5**, 176-180 (2021).
9. J. Cernicharo, M. Agúndez, R. Kaiser, C. Cabezas, B. Tercero, N. Marcelino, J. Pardo, P. De Vicente, Discovery of two isomers of ethynyl cyclopentadiene in TMC-1: Abundances of CCH and CN derivatives of hydrocarbon cycles. *Astron. Astrophys.* **655**, L1 (2021).
10. A. M. Burkhardt *et al.*, Discovery of the pure polycyclic aromatic hydrocarbon indene (c-C_9H_8) with GOTHAM observations of TMC-1. *Astrophys. J. Lett.* **913**, L18 (2021).
11. K. L. K. Lee, P. B. Changala, R. A. Loomis, A. M. Burkhardt, C. Xue, M. A. Cordiner, S. B. Charnley, M. C. McCarthy, B. A. McGuire, Interstellar detection of 2-cyanocyclopentadiene, C_5H_5CN, a second five-membered ring toward TMC-1. *Astrophys.*

J. Lett. **910**, L2 (2021).

12. M. L. Sita *et al.*, Discovery of interstellar 2-cyanoindene (2-C_9H_7CN) in GOTHAM observations of TMC-1. *Astrophys. J. Lett.* **938**, L12 (2022).
13. B. A. McGuire, A. M. Burkhardt, S. Kalenskii, C. N. Shingledecker, A. J. Remijan, E. Herbst, M. C. McCarthy, Detection of the aromatic molecule benzonitrile (c-C_6H_5CN) in the interstellar medium. *Science* **359**, 202-205 (2018).
14. A. M. Burkhardt, R. A. Loomis, C. N. Shingledecker, K. L. K. Lee, A. J. Remijan, M. C. McCarthy, B. A. McGuire, Ubiquitous aromatic carbon chemistry at the earliest stages of star formation. *Nat. Astron.* **5**, 181-187 (2021).
15. B. A. McGuire *et al.*, Detection of two interstellar polycyclic aromatic hydrocarbons via spectral matched filtering. *Science* **371**, 1265-1269 (2021).
16. M. Agúndez, C. Cabezas, B. Tercero, N. Marcelino, J. Gallego, P. de Vicente, J. Cernicharo, Discovery of the propargyl radical (CH_2CCH) in TMC-1: One of the most abundant radicals ever found and a key species for cyclization to benzene in cold dark clouds. *Astron. Astrophys.* **647**, L10 (2021).
17. M. Agúndez, N. Marcelino, C. Cabezas, R. Fuentetaja, B. Tercero, P. de Vicente, J. Cernicharo, Detection of the propargyl radical at λ 3 mm. *Astron. Astrophys.* **657**, A96 (2022).
18. J. Cernicharo *et al.*, Discovery of CH_2CHCCH and detection of HCCN, HC_4N, CH_3CH_2CN, and, tentatively, CH_3CH_2CCH in TMC-1. *Astron. Astrophys.* **647**, L2 (2021).
19. W. D. Langer, F. P. Schloerb, R. L. Snell, J. S. Young, Detection of deuterated cyanoacetylene in the interstellar cloud TMC 1. *Astrophys. J.* **239**, L125-L128 (1980).
20. J. Cernicharo, N. Marcelino, M. Agúndez, C. Bermúdez, C. Cabezas, B. Tercero, J. Pardo, Discovery of HC_4NC in TMC-1: A study of the isomers of HC_3N, HC_5N, and HC_7N. *Astron. Astrophys.* **642**, L8 (2020).
21. Y. C. Minh, W. M. Irvine, Upper limits for the ethyl-cyanide abundances in TMC-1 and L134N: Chemical implications. *Astrophys. Space Sci.* **175**, 165-169 (1991).
22. J. Cernicharo, R. Fuentetaja, C. Cabezas, M. Agúndez, N. Marcelino, B. Tercero, J. R. Pardo, P. de Vicente, Discovery of five cyano derivatives of propene with the QUIJOTE line survey. *Astron. Astrophys.* **663**, L5 (2022).
23. M. Agúndez, N. Marcelino, B. Tercero, J. Cernicharo, Aromatic cycles are widespread in

cold clouds. *Astron. Astrophys.* **677**, L13 (2023).

24. C. Cabezas, I. Peña, J. Cernicharo, Laboratory rotational spectroscopy and astronomical search of ethynyl substituted naphthalene. *Mon. Not. R. Astron. Soc.* **519**, 2590-2597 (2023).
25. S. S. Prasad, W. T. Huntress Jr, A model for gas phase chemistry in interstellar clouds. I-The basic model, library of chemical reactions, and chemistry among C, N, and O compounds. *Astrophys. J., Suppl. Ser.* **43**, 1-35 (1980).
26. R. Gredel, S. Lepp, A. Dalgarno, E. Herbst, Cosmic-ray-induced photodissociation and photoionization rates of interstellar molecules. *Astrophys. J.* **347**, 289-293 (1989).